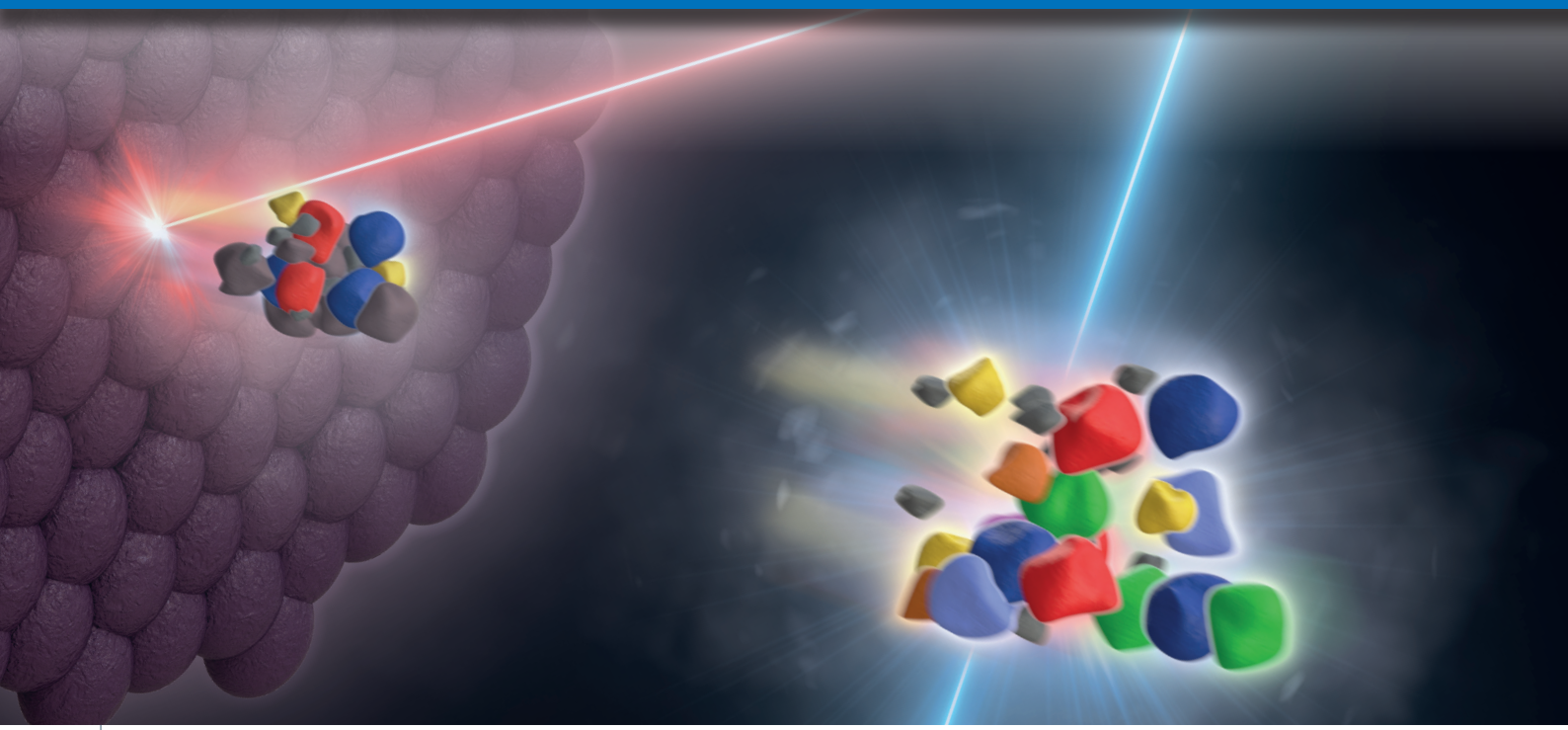

MALDI-2 for enhanced *in situ N*-glycan analysis

N-glycans are important players in a variety of pathologies including different types of cancer, (auto)immune diseases, and also viral infections.

Abstract

Matrix-assisted laser desorption/ionization mass spectrometry (MALDI-MS) is an important tool for high-throughput *N*-glycan profiling and, upon use of tandem MS, for structure determination. By use of MALDI-MS imaging (MSI) in combination with PNGase F treatment, also spatially-correlated *N*-glycan profiling from tissue sections becomes possible. Here we coupled laser-induced postionization, or MALDI-2, to a trapped ion mobility quadrupole time-of-flight mass spectrometer (timsTOF fleX MALDI-2, Bruker Daltonics). We demonstrate that negative ion mode MALDI-2-MSI is capable of providing high quality *N*-glycan tissue distributions. Combined with the advantageous fragmentation behavior of $[M-H]^-$ ions, exceedingly rich structural information on the composition of complex *N*-glycans was moreover obtained directly from thin tissue sections of human cerebellum and upon use of low-energy collision-induced dissociation tandem MS. Providing a complete package for MS-based glycan research, MALDI-2 will become a valuable tool in glycobiology research.

Keywords: timsTOF fleX MALDI-2, MALDI-2, N-glycans, oligosaccharides, imaging

Authors: Bram Heijs[1], Jens Soltwisch[2], Klaus Dreisewerd[2];
[1] Leiden University Medical Center; [2] University of Münster

Introduction

N-linked glycosylations, or *N*-glycans, are a class of common oligosaccharide post-translational protein modifications. They serve as important molecular modulators of the communication of a cell with its direct and indirect environment. Altered glycosylation has been associated with a variety of pathologies, including various types of cancer as well as response to treatment strategies, and disease progression like metastasis [1-5].

Matrix-assisted laser desorption/ionization mass spectrometry (MALDI-MS) is a common and much exploited tool for the analysis of *N*-glycans that are chemically or enzymatically released from their carrier proteins [6-8]. Methods utilizing positive ion mode (+) MALDI provide good sensitivity for the detection of alkali-metal adducts of *N*-glycans, but provide limited structural information in tandem MS applications. Negative ion mode (-) detection of deprotonated species provides unique structural information, but lacks sensitivity due to extensive in-source dissociation (ISD) of the produced ions [9-11]. More recently, *in situ* analysis of *N*-glycans directly from tissue sections has been enabled by MALDI-MS imaging (MALDI-MSI). Partly due to the limited sensitivity of the negative ion mode, *N*-glycan MALDI-MSI has so far only been reported in positive ion mode, and structural information was always obtained through orthogonal analyses of tissue extracts [12-14].

When MALDI-2 (or MALDI combined with laser-induced postionization) was introduced by Soltwisch *et al.* in 2015 [15] they showed increased ion yields for disaccharides in negative ion mode. This finding instigated our here presented study onto the feasibility of *N*-glycan analysis by (-)MALDI-2-MSI.

How to Perform (-)MALDI-2-MSI of *N*-glycans

Full experimental details including a comprehensive study onto the fundamentals of (-)MALDI-2-MS of oligosaccharides have been described in detail, recently [16]. Only the most relevant experimental aspects are summarized here. Formalin-fixed and paraffin-embedded (FFPE) human brain tissue (cerebellum) from a 79-year-old subject was sectioned at 5 μm thickness and mounted on standard microscope glass slides. Sections were dewaxed and consecutively rehydrated using xylene and an ethanol-to-water gradient. The endoglycosidase PNGase F was homogeneously applied to the tissue using an automated spray robot. The enzymatic reaction was incubated overnight at 37°C in a saturated humid environment. For negative ion mode analysis nor-harmane was used as the MALDI matrix and applied using the sprayer at 41 mM concentration in 50:50 acetonitrile:deionized water (%v/v). For the control analyses (on consecutive sections) in positive ion mode, 46 mM 2,5-dihydroxyacetophenone in 50:50 acetonitrile:deionized water (%v/v) was used as MALDI matrix. Both matrices were mixed with 5 µM maltoheptaose, which served as internal standard for intensity normalization.

(-)MALDI-2-MSI was performed on the timsTOF fleX MALDI-2 (Bruker Daltonics, Bremen, Germany, [17]) at optimized conditions [16]: N_2 cooling gas pressure (p), 3.0 mbar; MALDI laser pulse energy, 34 μJ; interlaser pulse delay (τ), 30 μs; MALDI-2 laser pulse energy, 350 μJ; 50 laser shots per pixel. (+)MALDI-MSI analysis was performed on the same timsTOF flex MALDI-2 instrument at optimized settings: p, 3.0 mbar; MALDI laser pulse energy, 34 μJ; 500 laser shots per pixel. Spectra were recorded using a 1 kHz repetition rate for both MALDI and MALDI-2 lasers, and over an *m/z* range between 900-3000, using a 50 × 50 μm^2 pixel size ("M5 small"). Following the MSI analysis, data were loaded into SCiLS Lab MVS (v. 2020a Pro, Build 8.00.11593, SCiLS Lab/Bruker Daltonics).

Results and discussion

N-glycan MALDI-2-MSI

The current 'gold standard' method for *N*-glycan MALDI-MSI is based on the detection of alkali-metal adducts (predominantly sodiated species) in positive ion mode. Therefore, analysis of deprotonated species in (-)MALDI-2-MSI was compared to the 'gold standard' method to assess whether the same *N*-glycans would be observed, and if they would have similar relative intensities and reflect the same spatial distributions of the species in brain tissue. Figure 1A shows two representative mass spectra obtained from the two analyses. Due to the previously mentioned ISD in the negative ion mode, there seems to be a slight bias towards the smaller *N*-glycans in the (-)MALDI-2-MSI analysis (for more details, see [16]). The affected glycans with an intensity variation of more than >±10% are highlighted in the spectrum. However, as can be deduced from Figure 1B-I, the recorded distributions showed the same glycans to be present in similar morphological areas upon measurement with the two ion polarities. It should be noted that (+)MALDI-2-MS of oligosaccharides was also attempted, but did not result in gains in ion yield as observed in the negative ion mode [16].

One striking observation is that the majority of the registered *N*-glycans has very similar expression profiles across the investigated brain area (Figure 2). To make sure the

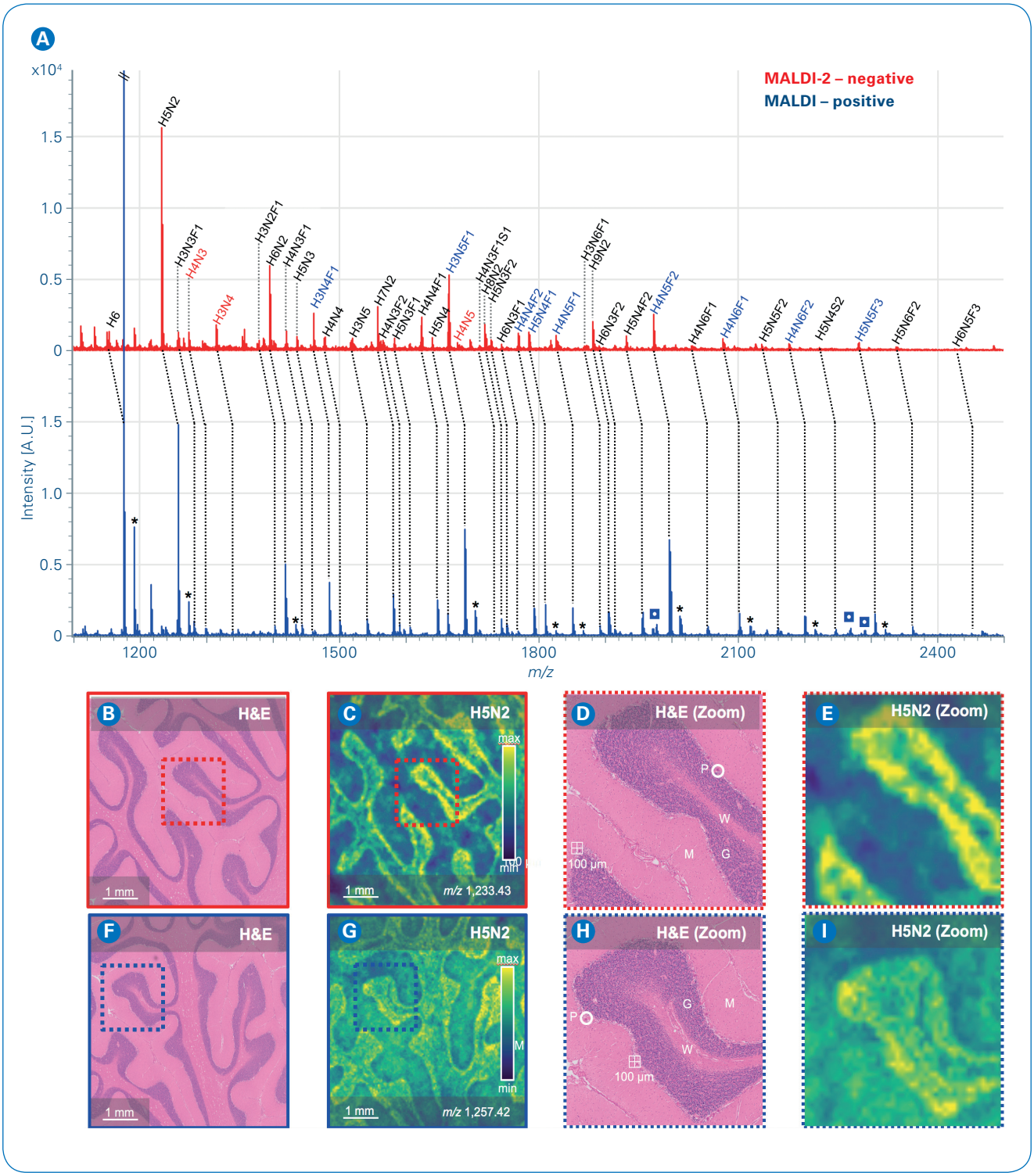

Figure 1: Spectra and images of positive ion mode MALDI-MSI and negative ion mode MALDI-2-MSI. (A) Average spectra for negative ion mode MALDI-2-MSI (red) and positive ion mode MALDI-MSI (blue) with assigned N*-glycan species. Colored* N*-glycan compositions represent a >±10% variation of intensity between positive and negative ion mode analyses. Peaks with an asterisk (*) in the positive ion mode spectrum are potassium adducts. (B), (F) H&E-stained consecutive section displaying cerebellar brain morphology using a standard staining protocol. (C), (G) Example ion images for* N*-glycan H5N2 in human cerebellum. (D), (H) Zoom-in on the histology with different morphological structures annotated (P – Purkinje cell, G – granular layer, M – molecular layer, W – white matter). (E), (I) Zoom-in on example H5N2 images. In red, (-)MALDI-2-MSI images, and in blue, (+)MALDI-MSI images.*

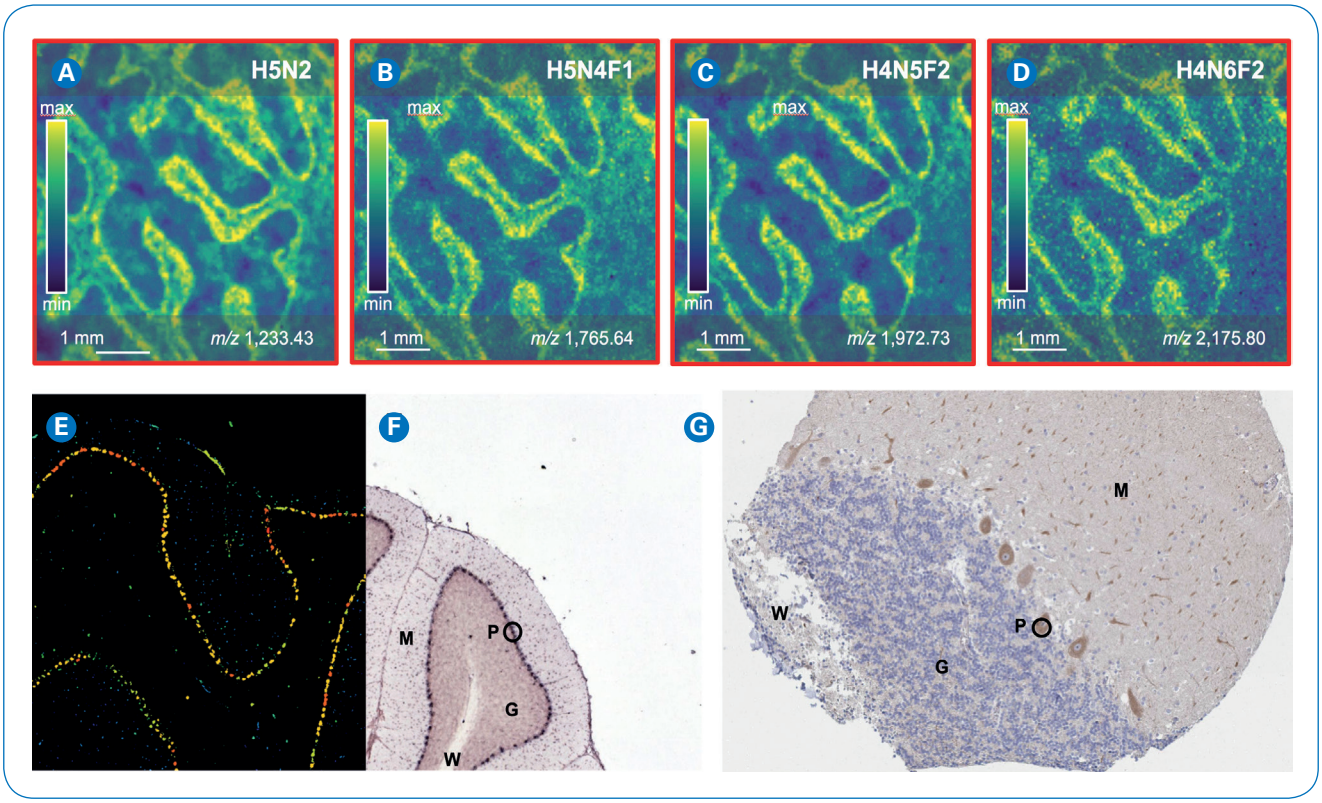

Figure 2: Example images of various N*-glycan species in the human cerebellum.* Ⓐ-Ⓓ *In red squares the images obtained using (-)MALDI-2-MSI of the human cerebellum, and in* Ⓔ-Ⓖ *the expression of the mannosidase 1, alpha (*man1a1*) enzyme in mouse brain (*Ⓔ*, expression profiling;* Ⓕ*,* in situ *hybridization) and human (54 y/o male) brain (*Ⓖ*, immunohistochemistry) obtained from the Allen Mouse Brain atlas (http://www.brain-map.org) and the Human Protein Atlas (http://www.proteinatlas.org) respectively.* Man1a1 *expression occurs predominantly in the Purkinje cell layer (P) and the granular layer (G) of the brain, in comparison to the white matter (W) and molecular layer (M).* Man1a1 *is one of the enzymes of the* N*-glycan biosynthesis pathway. The enzyme is responsible for trimming a mannose residue from the H9N2 glycan to produce H8N2 in the endoplasmatic reticulum (ER).*

N-glycan expression was not biased by the analysis, resulting in similar images for all detected *N*-glycans, and to validate the overall expression of *N*-glycans in the cerebellum, the expression of mannosidase 1, alpha (*man1a1*) was assessed in the brain through the Human Protein Atlas (http://www.proteinatlas.org) and the Allen Mouse Brain Atlas (http://www.brain-map.org). We found *man1a1* to be predominantly expressed in the Purkinje cell layer in both human and mouse cerebellum. Additional expression was found in the granular layer, although at lower levels compared to the Purkinje cells. These findings correspond well to the distributions found for the *N*-glycans detected by MSI. In our view, these results show clearly that MALDI-2-MSI can be an exceedingly useful tool for the visualization of *N*-glycans in FFPE tissue sections.

In situ MALDI-2-MS/MS

In mass spectrometry-based glycomics, the negative ion mode is commonly used for obtaining tandem MS spectra, because these contain unique isomer-specific cross-ring fragment ion signals that are not readily available in the positive ion mode [18-19]. In previous MSI-based studies on *N*-glycans, oligosaccharide compositions were determined based on mass-matching, often in combination with the off-tissue analysis of extracts by MALDI-MS/MS [14]. This indirect and laborious approach is often required as the sensitivity of MALDI-MS/MS is generally too low for structure elucidation directly from tissue.

Here we show that with the timsTOF fleX MALDI-2 advancements are achieved for on-tissue MS/MS of *N*-glycans. In total, the identity of 14 out of the 38 tentatively assigned *N*-glycan species as observed in the (-)MALDI-2-MSI analysis (Figure 1) was confirmed by (-)MALDI-2-MS/MS directly from the post-MSI analyzed tissue section. Figure 3 shows an example of an on-tissue MS/MS spectrum from H5N2, obtained using MALDI-2 in the negative ion mode.

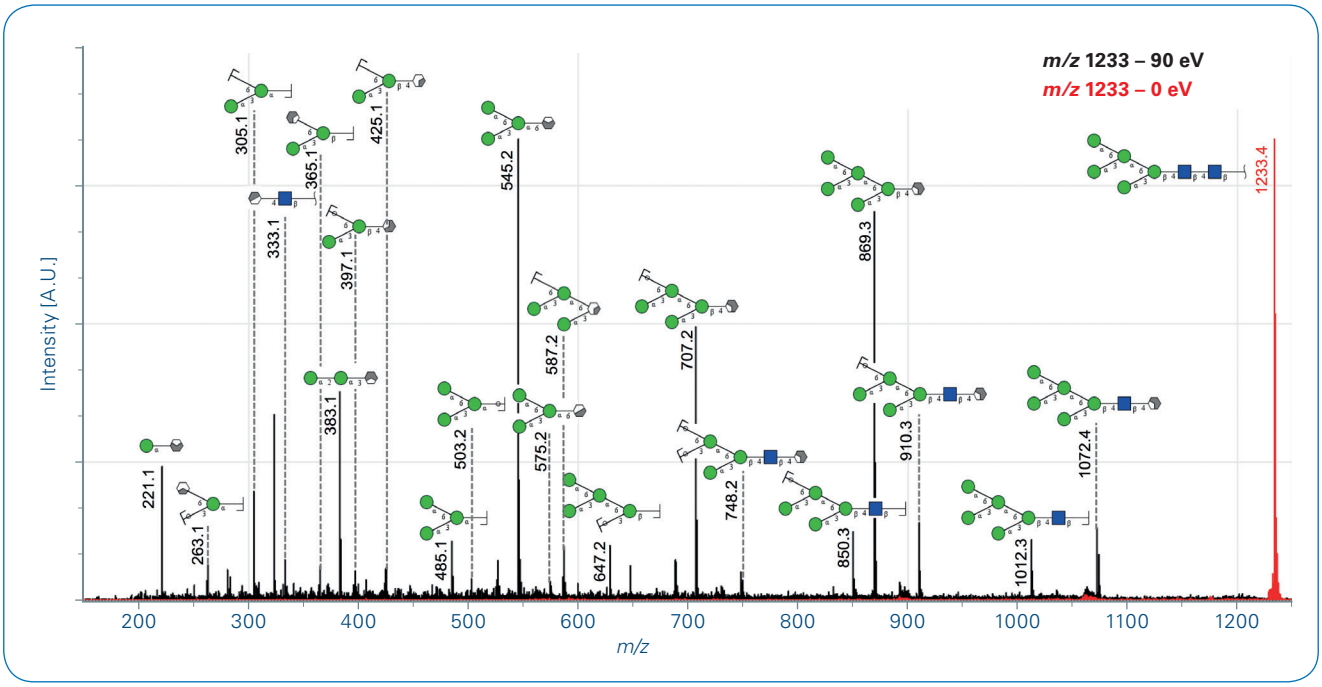

Figure 3: MALDI-2 tandem MS spectrum of deprotonated H5N2 from human cerebellum. The red trace shows a pseudo-MS1 spectrum, where quadrupole filtering was applied but no collision energy (0 eV). The black trace shows the low-energy CID MS/MS spectrum that resulted by applying a collision energy of 100 eV (laboratory frame). Both spectra were acquired from a total of twenty 50 × 50 µm²-wide pixels from a human cerebellum tissue post-MSI analyzed by MALDI-2-MSI. Based on mass matching (mass error tolerance, ±10 ppm), the majority of high intensity peaks could be assigned with fragment identities. Note that the applied method, which is not incorporating the use of ion mobility spectrometry, does not allow for separation of isomeric fragments. For visualization, only one hypothetical isomer is therefore denoted. Blue squares represent N-*acetylhexoses (HexNAc), green circles represent hexoses (Hex), and grey-ish hexagons represent various additional cross-ring fragments.*

Conclusion

MALDI-2 performed in the negative ion mode induces a boost in $[M–H]^-$ ion yields for the analysis of oligosaccharides. Using optimized conditions, we showed how the increased ion yields could be highly beneficial for the acquisition of high-quality MS/MS spectra and the structural analysis of *N*-glycans from minute sample amounts. In combination with the high quality MALDI-2-MSI of *N*-glycans from tissue, the timsTOF fleX MALDI-2 will be a valuable and complete tool for many applications in mass spectrometry-based glycomics research.

References

[1] Everest-Dass AV, Briggs MT, Kaur G, Oehler MK, Hoffmann P, Packer NH (2016). *N-glycan MALDI imaging mass spectrometry on formalin-fixed paraffin-embedded tissues enables the delineation of ovarian cancer tissues.* Mol. Cell. Proteomics. **15** (9), 3003–3016.

[2] Scott DA, Casadonte R, Cardinali B, Spruill L, Mehta AS, Carli F, Simone N, Kriegsmann M, Del Mastro L, Kriegsmann J, Drake RR (2019). *Increases in tumor N-glycan polylactosamines associated with advanced HER2-positive and triple-negative breast cancer tissues.* Proteom. Clin. Appl., **13**, 1800014.

[3] Briggs MT, Condina MR, Ho YY, Everest-Dass AV, Mittal P, Kaur G, Oehler MK, Packer NH, Hoffmann P (2019). *MALDI mass spectrometry imaging of early- and late-stage serous ovarian cancer tissue reveals stage specific N-glycans.* Proteomics. **19**, 1800482.

[4] Drake RR, McDowell C, West C, David F, Powers TW, Nowling T, Bruner E, Mehta AS, Angel PM, Marlow LA, Tun HW, Copland JA (2019). *Defining the human kidney N-glycome in normal and cancer tissues using MALDI imaging mass spectrometry.* J. Mass Spectrom. **55**, e4490.

[5] Heijs B, Holst-Bernal S, de Graaff MA, Briaire-de Bruijn IH, Rodriguez-Girondo M, van de Sande MAJ, Wuhrer M, McDonnell LA, Bovee JVMG (2020). *Molecular signatures of tumor progression in myxoid liposarcoma identified by N-glycan mass spectrometry imaging.* Lab. Invest.doi:10.1038/s41374-020-0435-2.

[6] Hall PL, Lam C, Alexander JJ, Asif G, Berry GT, Ferreira C, Freeze HH, Gahl WA, Nickander KK, Sharer JD, Watson CM, Wolfe L, Raymond KM (2018). *Urine oligosaccharide screening by MALDI-TOF for the identification of NGLY1 deficiency.* Mol. Genet. Metab. **124** (1), 82–86.

[7] Reiding KR, Bondt A, Hennig R, Gardner RA, O'Flaherty R, Trbojevic-Akmacic I, Shubhakar A, Hazes JMW, Reichl U, Fernandes DL, Pucic-Bakovic M, Rapp E, Spencer DIR, Dolhain RJEM, Rudd PM, Lauc G, Wuhrer M (2018). *High-throughput serum N-glycomics: method comparison and application to study rheumatoid arthritis andpregnancy-associated changes.* Mol. Cell. Proteomics. **18** (1), 3–15.

[8] Kotsias M, Kozak RP, Gardner RA, Wuhrer M, Spencer DIR (2019). *Improved and semi-automated reductive β-elimination workflow for higher throughput protein O-glycosylation analysis.* PLoS ONE. **14** (1), e0210759.

[9] Jovanovic M, Peter-Katalinić J (2016). *Negative ion MALDI-TOF MS, ISD, and PSD of neutral underivatized oligosaccharides without anionic dopant strategies, using 2,5-DHAP as a matrix.* J. Mass Spectrom. **51** (2), 111–122.

[10] Huang C, Yan J, Zhan L, Zhao M, Zhou J, Gao H, Xie W, Li Y, Chai W (2019). *Linkage and sequence analysis of neutral oligosaccharides by negative-ion MALDI tan-dem mass spectrometry with laser-induced dissociation.* Anal. Chim. Acta. **1071**, 25–25.

[11] Harvey DJ (2020). *Negative ion mass spectrometry for the analysis of N-linked glycans.* Mass Spectrom. Rev. **00**, 1–94.

[12] Powers TW, Neely BA, Shao Y, Tang H, Troyer DA, Mehta AS, Haab BB, Drake RR (2014). *MALDI imaging mass spectrometry profiling of N-glycans in formalin-fixed paraffin embedded clinical tissue blocks and tissue microarrays.* PLoS ONE. **9** (9), e106255.

[13] Powers TW, Holst S, Wuhrer M, Mehta AS, Drake, RR (2015). *Two-dimensional N-glycan distribution mapping of hepatocellular carcinoma tissues by MALDI-imaging mass spectrometry.* Biomolecules. **5** (4), 2554–2572

[14] Holst S, Heijs B, de Haan N, van Zeijl RJM, Briaire-de Bruijn IH, van Pelt GW, Mehta AS, Angel PM, Mesker WE, Tollenaar RA, Drake RR, Bovée JVMG, McDonnell LA, Wuhrer M (2016). *Linkage-specific in situ sialic acid derivatization for N-glycan mass spectrometry imaging from formalin-fixed paraffin-embedded tissues.* Anal. Chem. **88** (11), 5904–5913.

[15] Soltwisch J, Kettling H, Vens-Cappell S, Wiegelmann M, Müthing J, Dreisewerd K (2015). *Mass spectrometry imaging with laser-induced postionization.* Science. **348**, 211–215.

[16] Heijs B, Potthoff A, Soltwisch J, Dreisewerd K (2020). *MALDI-2 for the enhanced analysis of N-linked glycans by mass spectrometry imaging.* Anal. Chem. doi. 10.1021/acs.analchem.0c02732.

[17] Soltwisch J, Heijs B, Koch A, Vens-Cappell S, Höhndorf J, Dreisewerd K (2020). *MALDI-2 on a trapped ion mobility quadrupole time-of-flight instrument for rapid mass spectrometry imaging and ion mobility separation of complex lipid profiles.* Anal. Chem. **92**, 8697-8703.

[18] Harvey DJ, Scarff CA, Crispin M, Scanlan CN, Bonomelli C, Scrivens JH (2012). *MALDI-MS/MS with traveling wave ion mobility for the structural analysis of N-linked glycans.* J. Am. Soc. Mass Spectrom. **23** (11), 1955–1966.

[19] Harvey DJ (2005). *Fragmentation of negative ions from carbohydrates: part 2. Fragmentation of high-mannose N-linked glycans.* J. Am. Soc. Mass Spectrom. **16** (5), 631–646.

timsTOF fleX

MALDI 2 TECHNOLOGY

Enhanced Sensitivity and Coverage for SpatialOMx®

With the first enhancement in ionization technology in decades, SpatialOMx enabled timsTOF fleX with MALDI-2 represents an entirely unique and powerful solution for adding biological context to routine OMICS or pharma studies.

- Several orders of magnitude increase in sensitivity
- Higher information content that utilizes TIMS for enhanced peak capacity with MALDI Imaging
- Wide range of consumables and software supporting automation and providing more scientific insights

For more information please visit www.bruker.com/timstofflex

Learn More

You are looking for further Information?
Check out the link or scan the QR code.

www.bruker.com/timstofflex

For Research Use Only. Not for Use in Clinical Diagnostic Procedures.

Bruker Daltonics GmbH & Co. KG

Bremen · Germany
Phone +49 (0)421-2205-0

Bruker Scientific LLC

Billerica, MA · USA
Phone +1 (978) 663-3660

ms.sales.bdal@bruker.com – www.bruker.com